UC Irvine
UC Irvine Previously Published Works

Title

In vitro evolution of an HIV integrase binding protein from a library of C-terminal domain γS-crystallin variants

Permalink

Journal

ISSN

Authors

Moody, Issa S
Verde, Shawn C
Overstreet, Cathie M
et al.

Publication Date

DOI

Copyright Information

Peer reviewed

IN VITRO EVOLUTION OF AN HIV INTEGRASE BINDING PROTEIN FROM A LIBRARY OF C-TERMINAL DOMAIN γS-CRYSTALLIN VARIANTS

Issa S. Moody[a,†], **Shawn C. Verde**[b,†], **Cathie M. Overstreet**[a], **W. Edward Robinson Jr.**[b,*], and **Gregory A. Weiss**[a,c,*]

[a]Department of Molecular Biology & Biochemistry, University of California, Irvine Irvine, California 92697-2025, USA

[b]Department of Pathology and Laboratory Medicine, University of California, Irvine Irvine, California 92697-2025, USA

[c]Department of Chemistry, University of California, Irvine Irvine, California 92697-2025, USA

Abstract

A protein without natural binding functions was engineered to bind HIV-1 integrase. Phage display selections applied a library of variants based on the C-terminal domain of the eye lens protein human γS-crystallin. Multiple loop regions were altered to encode libraries with ≈3.6×10^{11} different variants. A crystallin variant, termed Integrase-Binding Protein-10 (IBP-10), inhibits integrase catalysis with nanomolar K_i values. IBP-10 interacts with the integrase C-terminal domain and inhibits integrase substrate affinity. This allosteric mechanism allows IBP-10 to inhibit drug resistant integrase variants. The results demonstrate the applicability of the crystallin scaffold for the discovery of binding partners and enzyme inhibitors.

Engineered protein scaffolds can offer affinity reagents to solve biomedical challenges.[1,2] Anti-HIV therapies, for example, require new binding partners, such as protein therapeutics, in response to the very high rate of viral mutagenesis and consequent acquisition of drug resistance by the virus.[3,4] Thus, developing alternative agents to target HIV proteins, such as integrase, could supplement and accelerate treatments for this ongoing pandemic.[5] Globally, >33 million people are infected with HIV, and ≈2 million people are killed each year by the virus.[6]

For protein-based, anti-viral compounds, the ideal scaffold for molecular recognition will exhibit the attributes of antibodies yet provide important advantages. Antibodies offer high affinity, solubility, specificity, and adaptable binding. However, the antibody scaffold is limited by its high cost, high molecular weight, low stability, and reducible disulfide bonds. Furthermore, new protein scaffolds could provide research tools for affinity purification, immuno-blotting and -precipitation, co-crystallization, inhibition, and sub-cellular localization. New classes of enzyme inhibitors could also provide powerful tools for controlling and studying protein function.

Previous reports demonstrate adapting the molecular recognition of proteins to new ligands and other targets.[7] For example, affibodies, based on the Z-domain of the IgG-binding Protein A from *Staphylococcus aureus*, have been used to identify inhibitors to the CD28-

*To whom correspondence should be addressed. ewrobins@uci.edu or gweiss@uci.edu.
†designates co-first authorship.

CD80 interaction.[8] Nanobodies, based on camel antibodies, have been tested in preclinical trials for the treatment of colorectal cancer and other diseases.[9,10] Maxibodies, single chain Fabs, have been used as agents against inflammation, cancer, and autoimmune diseases.[7] A paralog of human γS-crystallin, full-length γB-crystallin, has also been used as a scaffold for affinity reagent development; mutagenesis was applied to the affilins from γB-crystallin to alter the β-sheet regions of the protein.[11]

Of the major classes of crystallin, γS-crystallin offers particularly useful properties for affinity reagents. Expressed outside the eye lens in the cornea and retina, γS-crystallin has evolved for stability in different microenvironments.[12] Thus, γS-crystallin could be more resilient than α-, β-, or γA–F crystallins to different assays. The high solubility of γS-crystallin provides a useful property for developing affinity reagents. Such scaffold proteins must retain solubility, and could also prove useful for the solubilization of binding partners. Human γS-crystallin can remain soluble in physiological concentrations of 400 mg/ml (19.2 mM).[13] In addition, eye lens proteins are neither degraded nor re-expressed during the life of the organism. This long-term *in vivo* stability suggests variants of γS-crystallin could remain thermodynamically stable for prolonged durations.

Though its proposed physiological function is to maintain eye lens transparency,[14] γS-crystallin shares common structural features with antibodies (Fig. 1). These commonalities suggest an approach for engineering new molecular recognition capabilities into γS-crystallin. Notably, both proteins feature surface accessible loops, which antibodies apply to recognize antigens. Thus, γS-crystallin could provide adaptive binding surfaces to recognize a wide-range of antigens, analytes, or other targets.

The experiments in this report target HIV-1 integrase with variants of the C-terminal domain of the γS-crystallin protein scaffold (hereafter referred to as crystallin). Integrase is required for the establishment of productive HIV infections.[15] Thus, the protein is an excellent target for the development of affinity reagents. Multimeric integrase binds to substrate DNA, and catalyzes two steps of viral genome tailoring during the replication cycle: 3′-end processing (3′-EP) and strand transfer (ST).[15] 3′-EP begins after reverse transcription of the viral RNA into viral cDNA. In this process, multimeric integrase species bind to the termini of the nascent viral cDNA, and remove the two terminal nucleotides from each 3′-end. This 3′-EP reaction exposes 3′-OH groups for ligation into the host's DNA. After transport of the integrase-cDNA complex into the nucleus, multimeric integrase catalyzes the ST reaction with chromosomal DNA.[16] During ST, each processed 3′-OH nucleophilically attacks the phosphodiester backbone of the host DNA to allow insertion of the viral genome. From this inserted viral genome, transcription and translation of viral proteins and pre-proteins can proceed.[15]

Integrase can be divided into three domains, each with distinct functions.[17] The N-terminal domain (NTD), from residues 1–50, is responsible for binding viral DNA.[18,19] The core catalytic domain (CCD), from residues of 51-212, contains the active site of the enzyme.[19,20] Finally, the C-terminal domain (CTD), from residues 213-288, performs various roles, including host chromatin binding[21,22] and RT interaction.[23]

Both the 3′-EP and ST reactions catalyzed by integrase can be replicated through *in vitro* biochemical assays with purified, recombinant integrase and a radiolabeled DNA substrate homologous to the viral long terminal repeat sequence.[24] A third reaction, disintegration, which reverses DNA integration, can be performed *in vitro*, though the reaction has not been observed *in vivo*.[24,25] Catalysis of disintegration by integrase is used here and in other biochemical studies, because the reaction allows assay with severely attenuated integrase variants that do not produce detectable 3′-EP or ST products.[26]

A variety of small molecules and proteins can inhibit integrase.[27–29] Raltegravir (RGV) is FDA-approved for therapeutic use;[30] elvitegravir (EVG), exhibits improved efficacy but presently lacks FDA approval.[31] Unfortunately, as with all other HIV therapies, resistance to such inhibitors is inevitable, and can occur one to three months from the beginning of treatment.[4,32] Resistance to inhibitors can result from several mutations within the integrase core domain.[33] Other small molecule integrase inhibitors have been synthesized, but these inhibitors also directly compete with the substrate for binding to the active site of the enzyme.[28,34] Therefore, mutations conferring resistance to one class of inhibitors have been observed to grant resistance to other classes of molecules.[35]

Allosteric small-molecule inhibitors of integrase have been explored, and can provide micromolar levels of integrase inhibition. However, single residue mutations are sufficient to render these inhibitors ineffective.[36] Thus, non-small-molecule inhibitors and binding to integrase outside the core domain could provide new approaches to antiretroviral therapy. Proteins, for example, offer larger binding sites with a more diffuse hotspot of binding energy, which could prove more resilient to mutagenesis and the evolution of drug resistance.

Protein-based inhibitors of integrase include plant extract isolates such as MAP30 and GAP31,[37] monoclonal antibodies,[38] and peptides isolated from phage display.[39] One integrase-inhibitory peptide (amino acid sequence HCKFWW) can inhibit the ST reaction with a fifty percent inhibitory concentration (IC_{50}) value of 2 μM.[40] Other inhibitory peptides possess anti-integrase activity, though generally with higher IC_{50} values.[28] In addition to their micromolar potency, these peptides bind to the integrase active site, which could limit their usefulness against drug-resistant variants of integrase.[28] The monoclonal antibody mAb33 recognizes the C-terminal domain of integrase;[38] however, the antibody inhibits only the apoenzyme, and proved ineffective for integrase already bound to divalent metals, which are required by physiological integrase.[41] A peptide (amino acid sequence FHNHGKQ) identified from phage display inhibited the enzyme through binding to the catalytic core and C-terminal domains with a 70 μM IC_{50} value, though this peptide prevented only the ST reaction of the enzyme.[39]

In this report, we develop a new type of protein library for the discovery of inhibitors to integrase. Crystallin libraries were designed with peptides inserted into surface-exposed loops (Fig. 1) before selections for integrase affinity reagents. This strategy resulted in the identification of 12 ligands to integrase (Fig. 2A). In particular, IBP-10 could inhibit the three reactions catalyzed by integrase with nanomolar IC_{50} values (Fig. 3). The approach demonstrates the effectiveness of protein loop insertion into crystallin for the inhibition of integrase and potentially other proteins.

Library design focused on obtaining a small binding motif with flexibility for adapting its molecular recognition. Though not explored here, previous work has demonstrated the stability of the C-terminal domain of crystallin.[42] The phage-displayed library of crystallin variants was generated using site-directed mutagenesis as described previously with degenerate oligonucleotides designed to encode the libraries shown in Fig. 2.[43] Six independent crystallin libraries were constructed. Three libraries, programmed by the oligonucleotides C'CryLoop1C-CLib and C'CryLoop2C-CLib, encoded the peptide sequence $X_2CX_6CX_2$ (X = any amino acid) introduced into loop 1, loop 2, or both loops. Theoretical diversities of the resultant libraries were 4×10^{15}, 4×10^{15}, and 1.7×10^{31}, respectively. Two libraries, programmed by the oligonucleotides C'CryLoop1Lib and C'CryLoop2Lib, encoded either X_{13} or X_{14} peptide sequences in loops 1 or 2, respectively. There theoretical diversities were 8.2×10^{16}, and 1.6×10^{18}, respectively. The sixth library had X_{13} and X_{14} peptide sequences introduced into loops 1 and 2, respectively, for a

theoretical diversity of 1.3×10^{35}. The template for the oligonucleotide-directed mutagenesis was the gene encoding the C-terminal domain of crystallin (loop 1: residues 33-39; loop 2: residues 74-82) subcloned into the previously described phagemid vector pM1165a.[44] Initial tests confirmed effective display on the phage surface by this truncated crystallin variant. The low MW crystallin scaffold proved advantageous for selections, and its small size likely facilitated its effective display.

Twelve selectants from selection rounds 3 and 4 bound with high affinity to integrase (Fig. 2A). Two crystallin variants, IBP-1 and -2, were isolated from the $X_2CX_6CX_2$ library substituted in both loops 1 and 2. The remaining ten binders, IBP-3 through -12, were isolated from either the $X_2CX_6CX_2$ or the X_{13} library substituted in only loop 1. The relative binding affinities of the phage-displayed selectants varied >10-fold. Expression of the IBP variants not fused to the phage surface, quickly identified IBP-10 as a sequence with good yields from protein over-expression. For example, IBP-10 routinely yielded >20 mg/L of purified protein from bacterial expression, though further refolding and purification was required, which decreased overall yields. Therefore, subsequent experiments focused on the IBP-10 variant of crystallin.

First, the affinity to integrase by the over-expressed IBP-10 was examined by ELISA (Fig. 2B). IBP-10 binds to integrase with an apparent EC_{50} of 0.18 μM. Wild-type crystallin has weak affinity for integrase ($EC_{50} = 4.5$ μM), and provides a control for binding and inhibition studies. The protein-free, blocking solution (Thermofisher Scientific, Rockford, IL), negative control demonstrates the lack of affinity for the anti-integrase antibody to wild-type crystallin and IBP-10.

IBP-10 inhibited the 3′-EP, ST, and disintegration reactions catalyzed by integrase with nanomolar IC_{50} values, (Fig. 3, Table 1, and Supplementary Fig. S2–S4). Analogous to small molecule-based inhibition, the IC_{50} value for inhibition of the ST reaction catalyzed by integrase was 58% and 71% lower than the IC_{50} values for the 3′-EP and disintegration reactions, respectively. Notably, these IC_{50} values are only three-fold higher than the IC_{50} values obtained for the FDA-approved ST-inhibitor, RGV (Supplementary Table S2). The control, wild-type crystallin, exhibited approximately 10-fold higher IC_{50} values for the three reactions. As expected for the negative control, BSA failed to inhibit the three reactions catalyzed by integrase.

Next, integrase variants resistant to inhibition by RGV, EVG, or other integrase inhibitors were assayed for catalysis of the disintegration reaction in the presence of IBP-10 (Table 2). Though RGV and EVG do not inhibit disintegration catalysis, the active site location of most RGV- and EVG-resistant integrase mutations can nearly eliminate catalytic activity;[26,32] thus, only the robust disintegration reaction was examined for inhibition by IBP-10. IBP-10 inhibited RGV-resistant integrase and reference integrase with similar IC_{50} values. In contrast, the RGV-resistant G140S+Q148H variant of integrase can necessitate a >200-fold increase in RGV concentration for inhibition.[33] C-terminal domain mutants, many of which were identified through previous RGV- or EVG-mediated selection of HIV within the Robinson lab (data not shown), were also susceptible to disruption by IBP-10.

Integrase binding to DNA in the presence of IBP-10 was next examined using a substrate affinity assay (Table 1 and Supplementary Fig. S5). IBP-10 blocked integrase binding to the DNA substrate. Wild-type crystallin also inhibited integrase binding to DNA with IC_{50} values >30-fold higher than required by IBP-10. The negative control, BSA, failed to inhibit integrase binding to DNA.

To identify the region of integrase required for binding to IBP-10, truncation constructs of integrase were assayed for the catalysis of the disintegration reaction (Table 3). These N- or

C-terminal domains of integrase fused to the catalytic core domain constructs are severely attenuated for the 3′-EP or ST reactions (Supplementary Table S3) due to reduced dimerization and tetramerization.[21] Additionally, the truncation constructs of integrase were tested for binding to DNA in the presence of IBP-10. IBP-10 was unable to inhibit disintegration catalysis by the integrase core fused to the N-terminal domain, although IBP-10 could inhibit catalysis of the disintegration reaction by the integrase core fused to the C-terminal domain. Furthermore, the IC_{50} value for the inhibition of disintegration by this C-terminal domain construct remained similar to the inhibition of full-length integrase. IBP-10 also inhibited DNA binding to the integrase core fused to the C-terminal domain, and again this inhibition had IC_{50} values similar to those of the full-length protein. The integrase core fused to the N-terminal domain was unable to bind DNA; therefore the effect of IBP-10 upon integrase binding could not be quantified for this construct.

To estimate the dissociation constant of the integrase-IBP-10 complex, the inhibition constant, K_i, was calculated using the Cheng-Prusoff method.[45] IC_{50} values derived from the 3′-EP, ST, and disintegration reactions were used to obtain K_i values of 0.40, 0.17, and 0.56 µM, respectively. The K_i values for inhibition match the IC_{50} values, which is consistent with competitive inhibition of DNA binding to integrase by IBP-10. The reported nanomolar K_i values ($< K_i > = 0.38$ µM) result from the high affinity interaction between IBP-10 and integrase.

The reported experiments demonstrate binding to HIV integrase by a selectant from a highly diverse library of phage-displayed crystallin variants. The approach complements small molecule inhibition of integrase, which includes several compounds in clinical trials and one FDA-approved drug. Unfortunately, HIV has acquired drug resistance to all approved antiretroviral therapies to date.[46] Thus, new therapeutic options could improve treatment strategies for HIV-infected individuals.

Principles from previously reported affinity reagents guided the choice of scaffold library for targeting integrase, and also suggested a new approach to library construction. Successful scaffolds must balance the requirements for altered sequence to provide new molecular recognition against the desirable characteristics of the wild-type protein, including stability, solubility, small size, and low production costs. Thus, our approach keeps the vast majority of the protein unaltered, and merely extends loops on the surface of the protein. This method seeks to conserve the key contacts required for successful scaffold folding and solubility. Unlike other elements of secondary structure, loops predominantly lack backbone hydrogen bonding. This property endows loops with greater mobility to accommodate a range of potential binding partners. The strategy is validated by loops used for antigen recognition by the Fab domains of antibodies[47] and also to engineer Fn3 binding activities by Koide and coworkers.[48] Furthermore, the successful acquisition of new binding affinity in a crystallin variant, without drastically altering the desirable properties, confirms the efficacy of our approach.

From the full-length, wild-type crystallin (20.8 kD), specific loops for mutagenic substitution were identified. First, the minimal folding domain could dramatically reduce the protein's MW, which offers the advantages of smaller size for protein expression and downstream applications. Thus, the C-terminal domain, previously described as a discrete, stable domain of crystallin, became the focus of our efforts.[42,49] The smaller size of the C-terminal domain of crystallin (10.5 kD) offers few obvious loops for mutagenesis and peptide insertion. Loops 1 and 2, which cover the top half of the protein, were identified as prime locations for mutagenesis (Fig. 1A). The two loops extend in the same direction, which could promote an avidity effect for the identification of high affinity binding partners and potential inhibitors. Parallel loops are also a notable feature of antibodies. Loops 1 and 2

included seven and nine residues, respectively, and were substituted with largely randomized sequences of 12 to 14 amino acids, to provide a wider range of structural and functional diversity. The peptide inserts included both randomized 13-mers and also $X_2CX_6CX_2$, a sequence often selected in phage display experiments with peptide libraries. The two sequences could thus explore both disulfide-constrained and potentially less rigid structures.

Of the twelve selectants identified from biopanning, only two possessed the non-wild-type sequence in both loops 1 and 2. Interestingly, no selectants encoded a mutagenically altered sequence in only loop 2. Though the loops appear to be in close proximity to one another in the wild-type crystallin structure, loop 1 could have better accessibility to potential binding partners, and therefore provide an advantage for binding to integrase. With loops 1 and 2 mutated, IBP-1 and -2 could benefit from an avidity effect to increase the binding affinity.

IBP-10 inhibits the three reactions catalyzed by integrase with nanomolar IC_{50} values, and also inhibits drug-resistant variants of integrase. Furthermore, the inhibitor exhibits selectivity for the physiologically relevant 3′-EP and ST reactions. At 121 residues, IBP-10 can provide the steric bulk required to simply block access to the active site. Experiments performed with integrase truncation constructs, however, demonstrate that IBP-10 does not bind to the active site of the enzyme. IBP-10 instead allosterically prohibits substrate binding and catalysis through binding directly to a composite surface consisting of the core and the C-terminal domains of integrase. Unlike mAb33, which also bound to the integrase C-terminal domain, IBP-10 inhibits the physiologically relevant metal-bound enzyme. The previously reported peptide ligands from phage display possess the limitations described above; in contrast, IBP-10 inhibits all reactions catalyzed by integrase. Such multi-pronged inhibition further suggests that IBP-10 interacts with multiple residues, which could reduce the potential for the development of inhibitor resistance from mutations to a single residue.

Due to the development of drug resistance, HIV has persisted as a pandemic for over three decades. Most treatments available for HIV-infected individuals target the essential viral enzymes: reverse transcriptase, protease, or integrase. New approaches to the inhibition of these proteins could counter drug resistance to antiretroviral therapy. The reported integrase inhibitor, IBP-10, has nanomolar IC_{50} values and selectivity for the integrase-catalyzed 3′-EP and ST reactions. Binding to the C-terminal domain of integrase targets a largely unexplored, but potentially quite important, binding site for allosteric inhibition of integrase catalysis. In addition, the approach could be applied to a wide range of HIV proteins and other pathogenic viruses.

Supplementary Material

Refer to Web version on PubMed Central for supplementary material.

Acknowledgments

References and notes

1. Huang J, Koide A, Makabe K, Koide S. Proc Natl Acad Sci U S A. 2008; 105:6578. [PubMed: 18445649]

2. Skerra A. J Mol Recognit. 2000; 13:167. [PubMed: 10931555]

3. Ricchetti M, Buc H. EMBO J. 1990; 9:1583. [PubMed: 1691709]

4. Baldanti F, Paolucci S, Gulminetti R, Brandolini M, Barbarini G, Maserati R. J Med Virol. 2010; 82:116. [PubMed: 19950236]

5. Lewin SR, Rouzioux C. AIDS. 2011; 7:885. [PubMed: 21422987]

6. UNAIDS. In Report on the global HIV/AIDS epidemic: Executive summary. Geneva: Joint United Nations Programme on HIV/AIDS; 2008. p. 45

7. Hey T, Fiedler E, Rudolph R, Fiedler M. Trends Biotechnol. 2005; 23:514. [PubMed: 16054718]

8. Sandstrom K, Xu Z, Forsberg G, Nygren PA. Protein Eng. 2003; 16:691. [PubMed: 14560055]

9. Stijlemans B, Conrath K, Cortez-Retamozo V, Van Xong H, Wyns L, Senter P, Revets H, De Baetselier P, Muyldermans S, Magez S. J Biol Chem. 2004; 279:1256. [PubMed: 14527957]

10. Cortez-Retamozo V, Backmann N, Senter PD, Wernery U, De Baetselier P, Muyldermans S, Revets H. Cancer Res. 2004; 64:2853. [PubMed: 15087403]

11. Ebersbach H, Fiedler E, Scheuermann T, Fiedler M, Stubbs MT, Reimann C, Proetzel G, Rudolph R, Fiedler U. J Mol Biol. 2007; 372:172. [PubMed: 17628592]

12. Sinha D, Esumi N, Jaworski C, Kozak CA, Pierce E, Wistow G. Mol Vis. 1998:4. [PubMed: 9485487]

13. Delaye M, Tardieu A. Nature. 1983; 302:415. [PubMed: 6835373]

14. Sun H, Ma Z, Li Y, Liu B, Li Z, Ding X, Gao Y, Ma W, Tang X, Li X, Shen Y. J Med Genet. 2005; 42:706. [PubMed: 16141006]

15. Craigie R. J Biol Chem. 2001; 276:23213. [PubMed: 11346660]

16. Pandey KK, Grandgenett DP. Retrovirology. 2008; 2:11. [PubMed: 19915684]

17. Craigie R, Bushman FD, Engelman A. EMBO J. 1993; 12:3269. [PubMed: 8344264]

18. Eijkelenboom A, van den End FMI, Vos A, Doreleijers J, Hard K, Tullius T, Plasterk RA, Kaptein R, Boelens R. Curr Biol. 1999; 7:739. [PubMed: 9368756]

19. Engelman A, Mizuuchi K, Craigie R. Cell. 1991; 67:1211. [PubMed: 1760846]

20. Engelman A, Englund G, Orenstein JM, Martin MA, Craigie R. J Virol. 1995; 69:2729. [PubMed: 7535863]

21. Chen JC, Krucinski J, Miercke LJW, Finer-Moore JS, Tang AH, Leavitt AD, Stroud RM. Proc Natl Acad Sci USA. 2000; 97:8233. [PubMed: 10890912]

22. Hare S, Gupta SS, Valkov E, Engelman A, Cherepanov P. Nature. 2010; 464:232. [PubMed: 20118915]

23. Wilkinson TA, Januszyk K, Phillips ML, Tekeste SS, Zhang M, Miller JT, Le Grice SFJ, Clubb RT, Chow SA. J Biol Chem. 2009; 284:7931. [PubMed: 19150986]

24. Chow SA. Methods Enzymol. 1997; 12:306.

25. Chow SA, Vincent KA, Ellison V, Brown PO. Science. 1992; 255:723. [PubMed: 1738845]

26. Greenwald J, Le V, Butler SL, Bushman FD, Choe S. Biochemistry. 1999; 38:8892. [PubMed: 10413462]

27. Hazuda DJ, Felock P, Witmer M, Wolfe A, Stillmock K, Grobler JA, Espeseth A, Gabryelski L, Schleif W, Blau C, Miller MD. Science. 2000; 287:646. [PubMed: 10649997]

28. Marchand C, Maddali K, Metfiot M, Pommer Y. Curr Top Med Chem. 2009; 9:1016. [PubMed: 19747122]

29. Reinke RA, Lee DJ, McDougall BR, Abrams H, King PJ, Victoria JG, Mao Y, Lei X, Reinecke MG, Robinson WE Jr. Virology. 2004; 326:203. [PubMed: 15302207]

30. Summa V, Petrocchi A, Bonelli F, Crescenzi B, Donghi M, Ferrara M, Fiore F, Gardelli C, Gonzalez Paz O, Hazuda DJ, Jones P, Kinzel O, Laufer R, Monteagudo E, Muraglia E, Nizi E, Orvieto F, Pace P, Pescatore G, Scarpelli R, Stillmock K, Witmer MV, Rowley M. J Med Chem. 2008; 51:5843. [PubMed: 18763751]

31. Shimura K, Kodama E, Sakagami Y, Matsuzaki Y, Watanabe W, Yamataka K, Watanabe Y, Ohata Y, Doi S, Sato M, Kano M, Ikida S, Matsuoka M. J Virol. 2008; 82:764. [PubMed: 17977962]

32. Malet I, Delelis O, Valantin M, Montes B, Soulie C, Wirden M, Tchertanov L, Paytavin G, Reynes J, Mouscadet J, Katlama C, Calvez V, Marcelin A. Antimicrob Agents Chemother. 2008; 52:1351. [PubMed: 18227187]

33. Da Silva D, Van Wesenbeeck L, Breilh D, Reigadas S, Anies G, Van Baelen K, Morlat P, Neau D, Dupon M, Wittkop L, Fleury H, Masquelier B. J Antimicrob Chemo. 2010; 6:1262.

34. Kobayashi M, Nakahara K, Seki T, Miki S, Kawauchi S, Suyama A, Wakasa-Morimoto C, Kodama M, Endoh T, Oosugi E, Matsushita Y, Murai H, Fujishita T, Yoshinaga T, Garvey E, Foster S, Underwood M, Johns B, Sato A, Fujiwara T. Antiviral Res. 2008; 80:213. [PubMed: 18625269]

35. Marinello J, Marchand C, Mott BT, Bain A, Thomas CJ, Pommier Y. Biochemistry. 2008; 47:9345. [PubMed: 18702518]

36. Al-Mawsawi LQ, Neamati N. ChemMedChem. 2011; 6:228. [PubMed: 21275045]

37. Lee-Huang S, Huang PL, Huang PL, Bourinbaiar AS, Chen H, Kung H. Proc Natl Acad Sci USA. 1995; 92:8818. [PubMed: 7568024]

38. Bizub-Bender D, Kilkosky J, Skalka AM. AIDS Res Hum Retrovir. 1994; 10:1105. [PubMed: 7530024]

39. Desjobert C, de Soultrait VR, Faure A, Parissi V, Litvak S, Tarrago-Litvak L, Fournier M. Biochemisty. 2004; 134:39.

40. Puras-Lutzke RA, Eppens NA, Weber PA, Houghten RA, Plasterk RHA. Proc Natl Acad Sci USA. 1995; 92:11456. [PubMed: 8524782]

41. Ramcharan J, Colleluori DM, Merkel G, Andrake MD, Skalka AM. Retrovirology. 2006; 310.1186/1742-4690-3-34

42. Purkiss AG, Bateman OA, Goodfellow JM, Lubsen NH, Slingsby C. J Biol Chem. 2002; 277:4199. [PubMed: 11706012]

43. Sidhu, SS.; Weiss, GA. In Phage Display: A Practical Approach. Lowman, HL.; Clackson, T., editors. Oxford University Press; 2004. p. 27-41.

44. Murase K, Morrison KL, Tam PY, Stafford RL, Jurnak F, Weiss GA. Chem Biol. 2003; 10:161. [PubMed: 12618188]

45. Cheng Y, Prusoff WH. Biochem Pharmacol. 1973; 22:3099. [PubMed: 4202581]

46. Pingen M, Nijhuis M, de Bruijn JA, Boucher CAB, Wensing AMJ. J Antimicrob Chemother. 2011; 66:1467. [PubMed: 21502281]

47. Al-Lazikani B, Lesk AM, Chothia C. J Mol Biol. 1997; 273:927. [PubMed: 9367782]

48. Koide A, Bailey CW, Huang X, Koide S. J Mol Biol. 1998; 284:1141. [PubMed: 9837732]

49. Wenk M, Herbst R, Hoeger D, Kretschmar M, Lubsen NH, Jaenicke R. Biophys Chem. 2000; 86:95. [PubMed: 11026675]
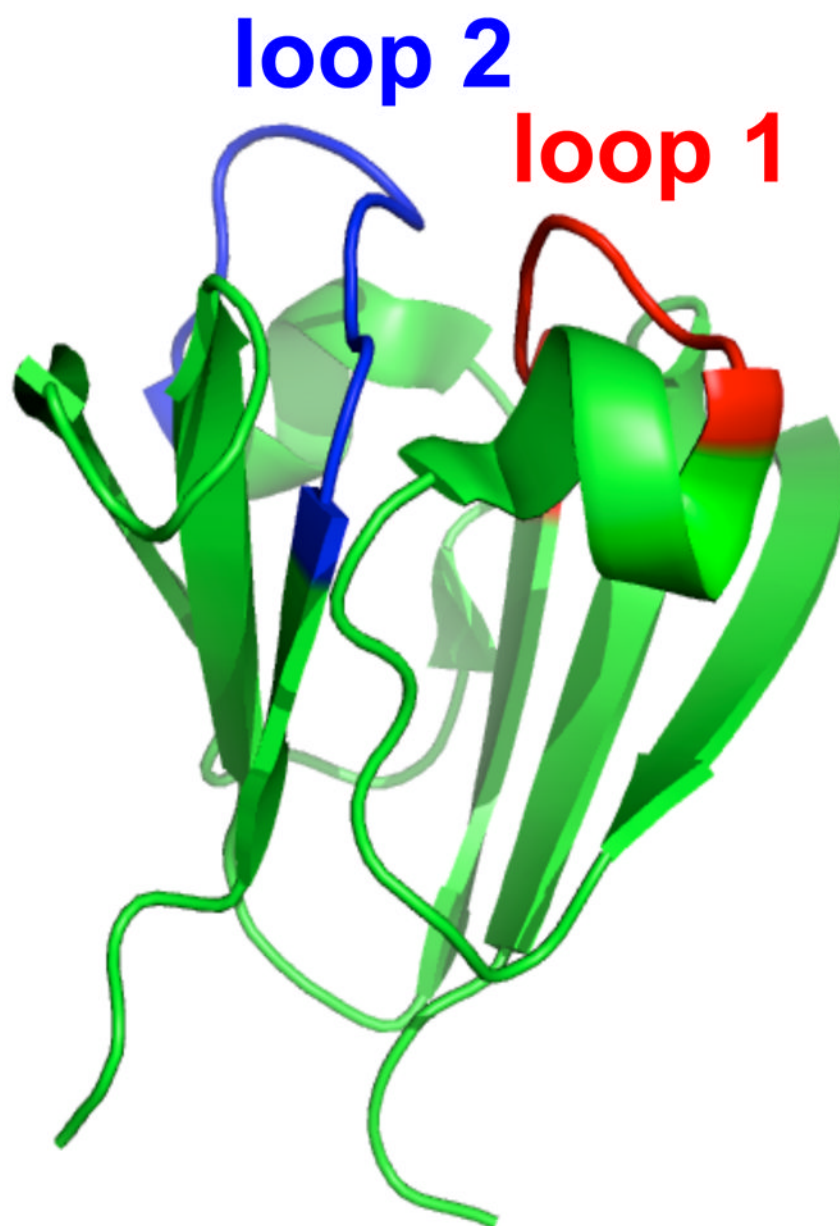
Fig. 1.
Structure of human C-terminal domain γS-crystallin. Two surface-exposed loops (red and blue) in the crystal structure of γS-crystallin (PDB: 1ha4) were targeted for mutagenesis. The loops' prime location for molecular recognition of target proteins suggested that crystallin could provide malleable, yet high affinity and specificity, binding reagents.
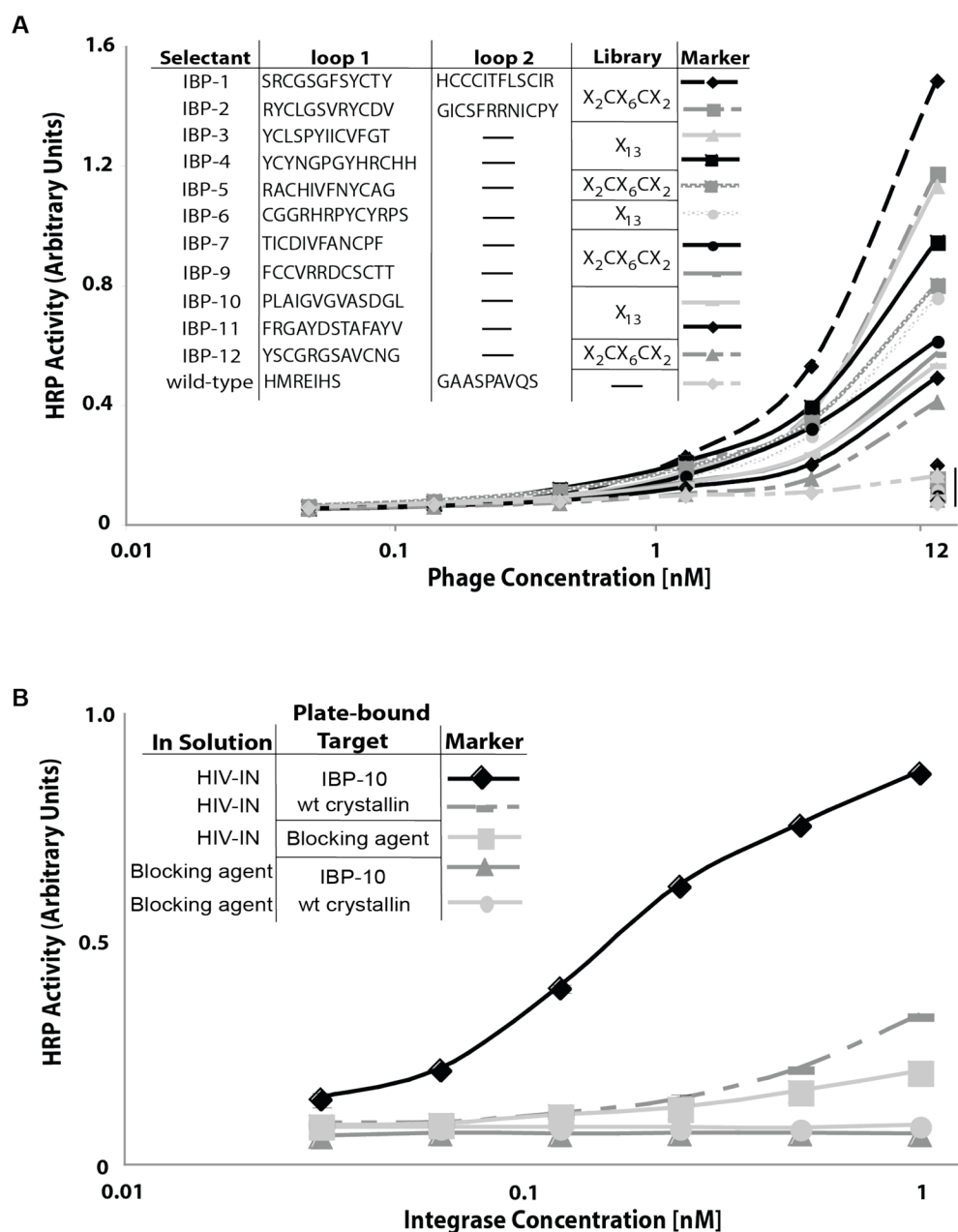
A

Selectant	loop 1	loop 2	Library	Marker
IBP-1	SRCGSGFSYCTY	HCCCITFLSCIR	$X_2CX_6CX_2$	
IBP-2	RYCLGSVRYCDV	GICSFRRNICPY		
IBP-3	YCLSPYIICVFGT	—	X_{13}	
IBP-4	YCYNGPGYHRCHH	—		
IBP-5	RACHIVFNYCAG	—	$X_2CX_6CX_2$	
IBP-6	CGGRHRPYCYRPS	—	X_{13}	
IBP-7	TICDIVFANCPF	—	$X_2CX_6CX_2$	
IBP-9	FCCVRRDCSCTT	—		
IBP-10	PLAIGVGVASDGL	—	X_{13}	
IBP-11	FRGAYDSTAFAYV	—		
IBP-12	YSCGRGSAVCNG	—	$X_2CX_6CX_2$	
wild-type	HMREIHS	GAASPAVQS	—	

B

In Solution	Plate-bound Target	Marker
HIV-IN	IBP-10	
HIV-IN	wt crystallin	
HIV-IN	Blocking agent	
Blocking agent	IBP-10	
Blocking agent	wt crystallin	

Fig. 2.
ELISAs of selectants from the crystallin library binding to integrase. *A.* Following selections, phage-based ELISAs identified crystallin variants with affinity for HIV-1 integrase. *B.* Upon over-expression and purification of non-phage-fused protein, IBP-10 exhibits high affinity for integrase. In both ELISAs, wild-type (wt) crystallin provides a negative control. In addition, the protein-free blocking agent negative control demonstrates lack of affinity for the anti-integrase antibody for binding to wild-type crystallin and IBP-10. The negative controls demonstrate that the depicted selectants fail to bind to BSA, used as a blocking agent. In *B*, the error bars (standard error, n=2) are quite small, but present.
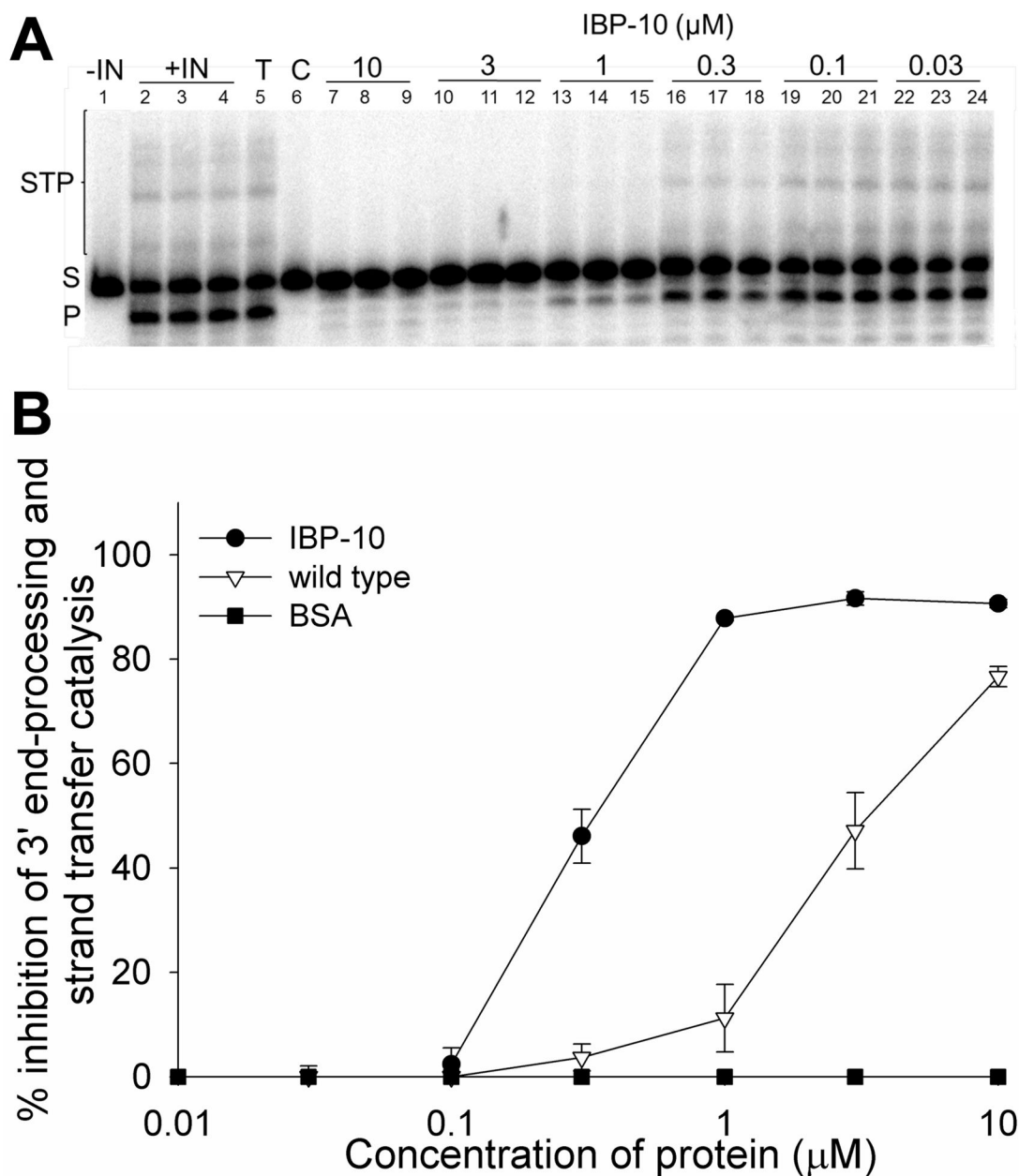
Fig. 3.
Inhibition of HIV-integrase mediated catalysis by IBP-10. *A*. In this urea-PAGE representative experiment, the addition of inhibition of the crystallin mutant, IBP-10, inhibits formation of integrase-mediated 3′-end processing products (P) and strand transfer products (STP) from radiolabelled oligonucleotide substrates (S). See Supplemental Fig. S2 for analogous gels of controls. Lane 1 provides a negative control for the reaction in the absence of integrase. The positive control, in triplicate, lanes 2–4, demonstrates the efficiency of the reaction in the absence of inhibitor. Lanes 5 and 6, respectively, provide negative and positive controls for integrase inhibition by L-tartaric acid (T), an inactive analog of the known inhibitor L-chicoric acid (C). Lanes 7–24 demonstrate inhibition by IBP-10 at the indicated concentrations of both 3′-end processing and strand transfer catalysis by integrase. *B*. Quantitative analysis of the inhibitory activities of IBP-10, its wild-type

variant, and the negative control (BSA). Results were analyzed via urea page and quantified via phosphorimager analysis. Results of reactions used to generate (B): IBP-10 (Panel A), wild-type, and BSA (Supplemental Fig. S2).

Table 1

IC$_{50}$ values (μM) of HIV-1 integrase inhibition by crystallin variants.

	3′-EP	**ST**	**Disintegration**	**DNA affinity**
IBP-10	0.40 (0.08)[a]	0.17 (0.01)	0.57 (0.01)	0.27(0.01)
wild-type	3.81 (0.43)	1.76 (0.82)	4.45 (0.19)	8.23(1.39)
BSA	_b	_b	_b	_b

[a]Standard error is indicated in parentheses (n=3).

[b]No inhibition observed at the experimental concentrations.

Table 2

IC$_{50}$ values (μM) of mutant[a] HIV-1 integrase disintegration activity inhibition by IBP-10.

	IC$_{50}$	Fold change	Mutant integrase selected by
Reference	0.140 (0.01)[b]	—	—
G140A+Q148H	0.190 (0.03)	1.35	RGV
G140S+Q148H	0.090 (0.01) [†]	0.5	RGV
N155H	0.400 (0.11) [†]	2.85	RGV
R224Q	0.080 (0.02) [†]	0.57	—[c]
R262K	0.240 (0.02) [†]	1.7	—[c]
K264R	0.180 (0.02) [†]	1.3	RGV[c], EVG[c]
T66I+R263K+K266R	0.350 (0.07) [†]	2.5	EVG[c]

[a] Where appropriate, "+" refers to two or more mutations present within the same integrase variant.

[b] Standard error is indicated in parentheses (n=3).

[c] Robinson lab unpublished results; mutations observed within integrase genes of inhibitor-resistant virus isolated from RGV-, EVG-, or other inhibitor-treated cell cultures.

[†] Denotes significantly altered values with $p < 0.05$.

Table 3

DNA affinity and IC_{50} values (μM) for IBP-10 inhibition of integrase activity by full-length reference integrase and N- and C-terminal integrase domains fused to the integrase core catalytic domain (core).

	DNA affinity	Disintegration
Reference	0.27 (0.01) [c]	0.57 (0.01)
N-term+Core	_a	_b
Core+C-term	1.83 (0.18)	0.17 (0.05)

[a] Substrate affinity below detectable limits.

[b] No inhibition observed at the experimental concentrations.

[c] Standard error is indicated in parentheses (n=3).